Article published online: 2023-09-19

Unveiling the Enigma of Sellar and Parasellar Pathologies: A Pictorial Essay

Anshika Gulati[1]

[1] Department of Radiology & Imaging, Ram Manohar Lohia Hospital, Delhi, India

Indographics 2022;1:116–125.

Address for correspondence Anshika Gulati, MD, Department of Radiology & Imaging, Ram Manohar Lohia Hospital, Connaught Place, Delhi 110001, India (e-mail: drgulatianshika@gmail.com).

Abstract

Sellar and parasellar pathologies often present with nonspecific symptoms. Clinical examination and endocrine studies are useful but cross-sectional imaging is indispensable to characterize and accurately localize the lesion. Magnetic resonance imaging with its multiplanar capability and excellent soft tissue contrast resolution is workhorse in evaluation of sellar and parasellar pathologies. Imaging findings of a broad spectrum of lesions is presented in this article along with anatomy and literature review.

Keywords

- magnetic resonance imaging
- pituitary
- sella turcica

Introduction

Sellar region is a complex area of the brain housing the master endocrine gland adorning its bony throne, sella turcica, surrounded by an army of other important structures, any of which can give rise to pathologies ranging from incidental to potentially fatal. Most of these lesions present with hypopituitarism, visual disturbances, headache, and projectile vomiting due to obstructive hydrocephalus, cognitive disturbance, or failure to thrive. These symptoms are nonspecific, occurring due to mass effect on parasellar structures rather than due to any particular lesion. So differentiating among these lesions on the basis of clinical presentation alone is not always possible. Nonetheless, the management of each of these lesions differs considerably. Radiological assessment is of utmost importance in reaching a definitive diagnosis thereby aiding in formulation of an appropriate management strategy. Magnetic resonance imaging (MRI) is the imaging investigation of choice for sellar and parasellar pathologies owing to its multiplanar capability, superior soft tissue contrast resolution, and lack of ionizing radiation. It allows better demonstration of anatomy, localization and characterization of lesions, as well as assessment of their relationship with surrounding structures thereby helping to plan the surgical approach.

A Glimpse of Anatomy

Superior part of the basisphenoid houses pituitary gland in a midline concavity known as the sella turcica bounded anteriorly by anterior clinoid processes arising from lesser wing of sphenoid and posteriorly by dorsum sellae and posterior clinoid processes forming the superior border of clivus. Bony sella is lined by meninges on all sides leaving a small central opening (diaphragmatic hiatus) superiorly for transmitting the pituitary stalk. Superior to sella lies the suprasellar cistern which contains optic chiasm and pituitary stalk surrounded by the circle of Willis. Further superiorly lies the hypothalamus extending from lamina terminalis anteriorly to mammillary bodies posteriorly. Tuber cinereum is a part of hypothalamus located between the optic chiasm and mammillary bodies from which the infundibular stalk extends inferiorly, gradually tapering downwards. Superior to hypothalamus lies the third ventricle. Inferior to sella lies the sphenoid sinus which may be partially or completely aerated. Lateral to sella on either side lie dura-lined venous

DOI https://doi.org/10.1055/s-0042-1742580.

Thieme Medical and Scientific Publishers Pvt. Ltd., A-12, 2nd Floor, Sector 2, Noida-201301 UP, India

compartments known as cavernous sinuses (CSs). Through the CSs course the internal carotid artery (ICA) (cavernous segment) and VI cranial nerve (CN), while III, IV, V1, and V2 CNs lie within its lateral dural wall.[1]

Imaging Technique

Precontrast T1- and T2-weighted spin echo images are first acquired in coronal and sagittal planes using thin 3 mm slices, small field-of-view, and high-resolution matrix. This is followed by the dynamic and routine postcontrast images and delayed scanning after 30 to 60 minutes. A three-dimensional (3D) Fourier transformation gradient echo or fast/turbo spin echo sequence may be used for dynamic study. After a bolus injection of 0.05 to 1 mmol/kg intravenous gadolinium, six consecutive sets of three images are obtained in the coronal plane every 10 seconds.

Furthermore, a variety of advanced MRI techniques have been developed including 3D volumetric analysis of pituitary,[2] intraoperative MRI,[3] diffusion-weighted imaging (DWI),[4] MR spectroscopy (MRS),[5] and magnetization transfer ratio (MTR).[6]

Step-By-Step Approach

Sellar and parasellar pathologies may be classified according to etiology (normal variants, congenital, neoplastic, inflammatory, vascular, traumatic, etc.). Of the myriad lesions that can arise in sella and parasellar region, more than three-fourths are from among the "Big Five"' which include—adenoma, meningioma, aneurysm in adults, astrocytoma in children, and craniopharyngioma (CP) in both. All other lesions together account for less than 25% of parasellar pathologies.[7]

The goal of imaging is to localize and characterize the lesions as well as to delineate its entire extent, to aid in planning proper medical or surgical management. A step-by-step approach is suggested for complete evaluation and narrowing the differentials.

1. Localize: Begin by localizing the epicenter of the lesion to one of the four anatomical compartments, namely, intrasellar, suprasellar, parasellar, or infundibular stalk. Suprasellar lesions may arise from diaphragma sellae, optic chiasma, hypothalamus, or circle of Willis. Parasellar lesions arise from contents of CS—meninges, CNs, and blood vessels. Infrasellar lesions arise from nasopharynx. Various skull base lesions can involve the sella as well. Enlargement of the sella might suggest pituitary origin of the lesion. However, this is not always the case, as in case of empty sella, the sella turcica is enlarged but cerebrospinal fluid (CSF)-filled and pituitary itself is compressed to the floor of sella. If the pituitary gland cannot be identified separately from the lesion, then the pituitary itself is the site of origin.
2. Characterize: Look for intrinsic signal intensity of the lesion —solid/cystic/vascular, areas of hemorrhage/necrosis/calcification, and enhancement pattern.
3. Extension: Look for margins of the lesion—well circumscribed/infiltrating and describe relationships with surrounding structures.

Pituitary Adenoma

Pituitary adenoma is a benign neoplasm that arises from the adenohypophysis and is the most common intrasellar pathology.[8] Pituitary adenomas can be classified into micro, macro, or giant when they measure less than 1 cm, more than 1 cm, or more than 4 cm, respectively. Clinically, microadenomas present with hypersecretory syndromes while macroadenomas cause symptoms due to mass effect on adjacent structures.

Detection rate of pituitary microadenomas has increased manifold after introduction of dynamic contrast-enhanced MRI.[9] The enhancement of normal pituitary gland begins from the stalk, followed by pituitary tuft and finally there is centrifugal enhancement of the rest of the pituitary. Within 30 to 60 seconds, the entire gland shows homogenous enhancement followed by rapid washout. On the contrary, microadenomas show slow and gradual uptake of contrast with peak enhancement at 60 to 200 seconds that persists for a longer duration.[2] The maximum contrast difference between the normal pituitary tissue and microadenomas is attained approximately 30 to 60 seconds after the bolus injection of the intravenous contrast. Most microadenomas appear as relatively nonenhancing lesions within an intensely enhancing pituitary gland.[9] Delayed scan (30–60 minutes after contrast injection) may demonstrate a reversal of the image contrast obtained at 30 to 60 seconds on dynamic scanning. This is because the contrast from the normal

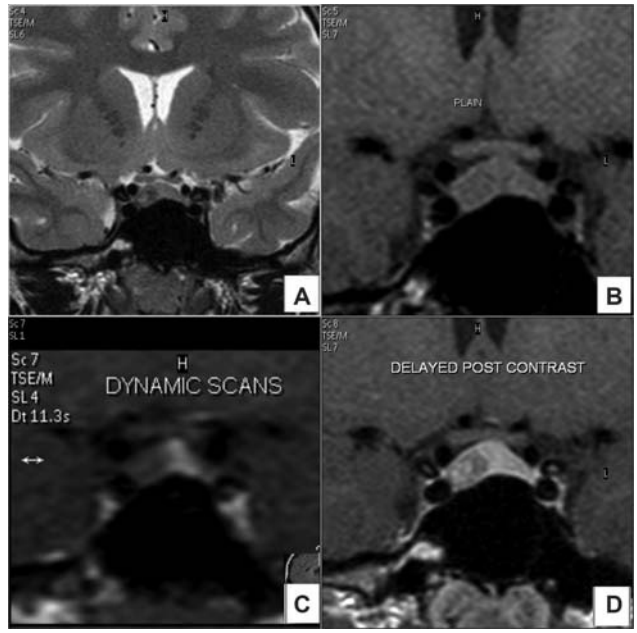

Fig. 1 Coronal T2-weighted image (T2WI) (**A**) and T1WI (**B**) of a patient presenting with amenorrhea and hyperprolactinemia show a right lateral pituitary lesion causing focal contour bulge and deviation of stalk. Dynamic contrast-enhanced coronal T1WI (**C**, **D**) show a pituitary microadenoma which enhances more slowly than the normal pituitary gland.

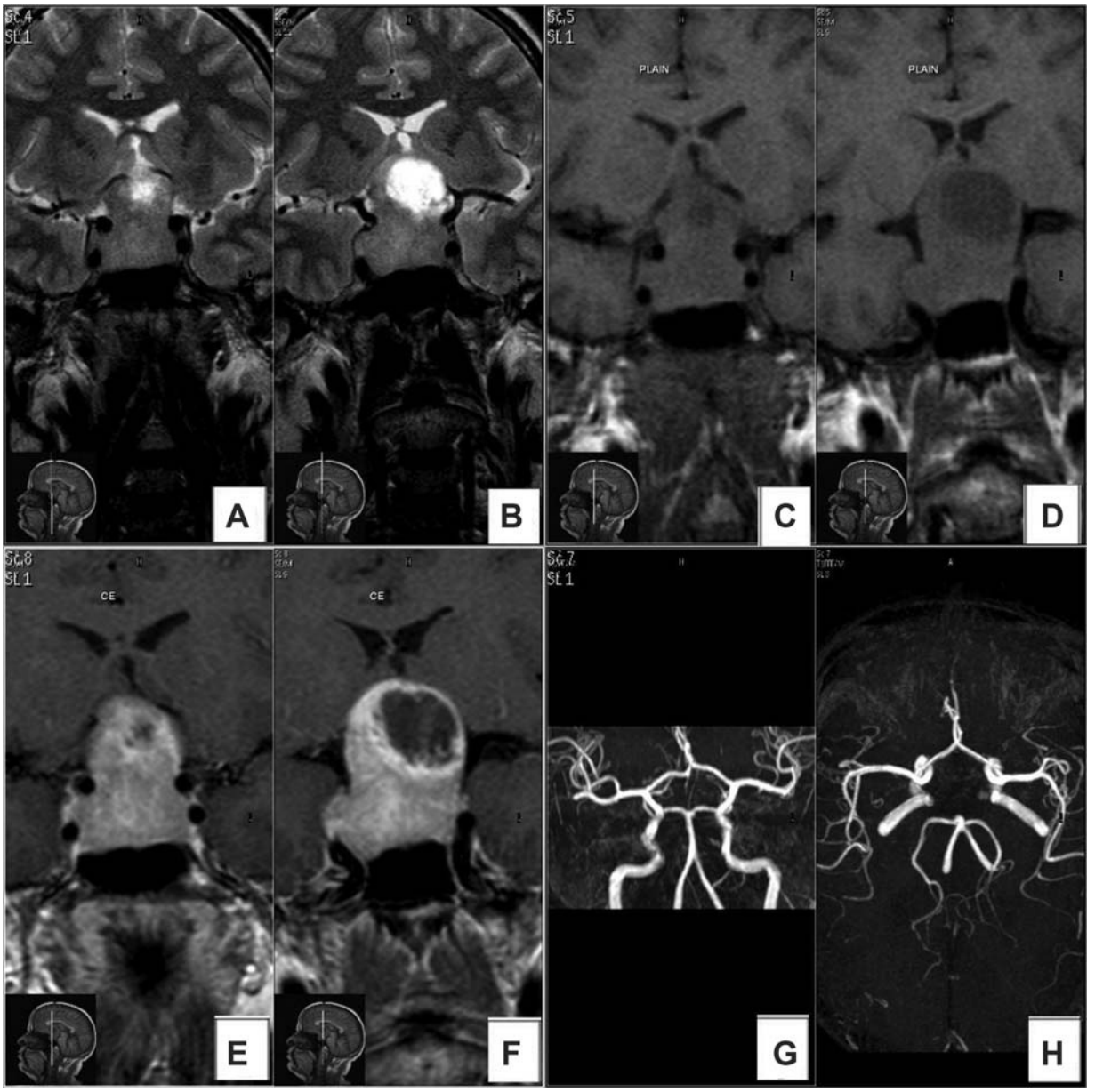

Fig. 2 In a 28-year-old lady presenting with headache and visual disturbance, coronal magnetic resonance (MR) images show a large lobulated "snowman" or "figure of 8" sellar and suprasellar lesion. Pituitary cannot be identified separately from this lesion suggesting macroadenoma. Areas of cystic degeneration are seen in the lesion superiorly toward the left. Solid component appears isointense on both T2-weighted image (T2WI) (**A**, **B**) and T1WI (**C**, **D**) and shows heterogeneous avid enhancement on postcontrast images (**E**, **F**). Superiorly, the lesion is compressing the optic chiasma and reaching up to the floor of third ventricle. Laterally, it shows cavernous sinus invasion, however, flow-void of internal carotid artery (ICA) is normal. Coronal (**G**) and axial (**H**) MR angio images show no e/o ICA stenosis.

pituitary gland fades but diffuses into the microadenoma which stands out as a hyperintense focus[10] (►**Fig. 1**).

Some microadenomas exhibit maximum lesion-to-gland contrast on unenhanced scans; however, this image contrast begins to diminish the moment the contrast-enhancing agent arrives in the pituitary gland. Some authors have even documented early enhancement in the microadenomas, long before the anterior lobe, which is attributed to pituitary adenomas having a direct arterial blood supply similar to that of posterior pituitary.[4]

A large heterogeneously enhancing sellar mass which cannot be identified separately from pituitary is a macroadenoma. It can show areas of hemorrhage and cystic change but usually no calcification (►**Fig. 2**). SIPAP (S, suprasellar, I, infrasellar, P, right and left parasellar, A, anterior, P, posterior) classification is a 6-figure number describing the extrasellar extension of pituitary adenomas.[11]

Suprasellar grading ranges from 0 to 4 where grade 0 adenoma does not bulge into suprasellar space, grade 1 bulges into the suprasellar cistern, grade 2 reaches up to the optical chiasma without displacing or stretching it, grade 3 when it displaces stretches the optic chiasm causing mass effect on third ventricle, and grade 4 adenoma obliterates one or both foramen of Monro resulting in hydrocephalus in lateral ventricles.

Infrasellar extension is graded from 0 to 2 where grade 0 refers to intact sellar floor, grade 1 refers to extension into sphenoid sinus, and grade 2 refers to extension beyond sphenoid sinus into nasopharynx inferiorly or ethmoid anteriorly.

For grading of parasellar extent of pituitary adenomas, Knosp–Steiner classification is used where three parallel lines, namely the medial tangent, intercarotid line, and lateral tangent drawn on cross-sections of intra- and supracavernous ICA, are used to define grades 0 to 4. Grade 0, 1, and 2 represents tumor extension up to the medial tangent, intercarotid line, and lateral tangent, respectively. Grade 3 corresponds to extension lateral-to-lateral tangential line and is further classified into 3a and 3b depending on whether it is superior or inferior to intracavernous ICA. Finally, grade 4 represents total encasement of cavernous ICA.[12]

Bulging of the lateral wall of the CS and lack of normal enhancement of the venous extrasellar spaces suggest CS invasion. Different anatomical classifications, based on MRI findings, have been proposed to specify if the CS is invaded by a pituitary tumor (PT). Some authors have suggested that an encasement of the ICA greater than 67% makes invasion certain while others suggested that an ICA remote from the sphenoid carotid sulcus is highly suggestive of CS invasion.[5]

Anterior grading ranges from 0 to 1 depending on extension into anterior cranial fossa with the landmark being an imaginary line drawn perpendicular to tuberculum sellae on sagittal section.

Posterior grading ranges from 0 to 1 depending on extension into prepontine cistern below the level of dorsum sellae on sagittal section.

Most of the pituitary adenomas are functioning tumors, majority being prolactinomas while 25% are nonfunctioning tumors.[13] This differentiation is crucial for management as prolactinomas are managed medically whereas nonfunctioning adenomas are treated by surgical excision. Magnetization transfer imaging is a recent advancement in MRI wherein tissue contrast is determined by the concentration of macromolecules and is quantified by MTR. In cases with hyperprolactinemia, the MTR value of prolactin-secreting adenomas is remarkably higher than the MTR of normal pituitary gland resulting in the high signal of prolactin-secreting adenomas on MT images. On the other hand, nonfunctioning adenomas have lower MTR values compared with normal pituitary gland accounting for their low signal on MTR images.[6]

Majority of pituitary adenomas are soft and hence easily resectable via minimally invasive endoscopic transsphenoidal approach, whereas some macroadenomas are hard due to increased fibrosis and are thus difficult to remove via endoscopic technique necessitating more extensive surgery. Pierallini et al demonstrated that soft adenomas have a low apparent diffusion coefficient (ADC) value of $(0.663 \pm 0.109) \times 10^{-3}$ mm^2/sec, whereas hard adenomas have a relatively high ADC value $(1.363 \pm 0.259) \times 10^{-3}$ mm^2/sec. Thus, preoperative knowledge of pituitary adenoma consistency may help the surgeon in deciding a proper surgical technique.[14]

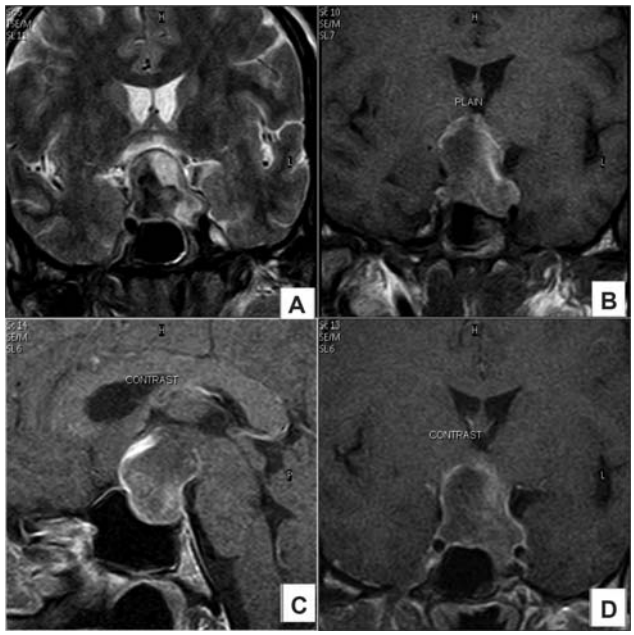

Fig. 3 Known case of pituitary macroadenoma on treatment with bromocriptine presented to emergency with sudden onset severe headache and visual disturbance. Coronal T2-weighted image (T2WI) and T1WI show that the mass is very heterogeneous in signal intensity with multiple hemorrhagic foci. Postcontrast sagittal (**C**) and coronal (**D**) images thin peripheral enhancement. These findings are consistent with pituitary apoplexy. Necrotic hemorrhagic macroadenoma was found at surgery.

Pituitary Apoplexy

Owing to their meager blood supply, pituitary adenomas may undergo infarction and hemorrhage and present acutely. This condition is referred to as pituitary apoplexy and can occur spontaneously or following therapy. These hemorrhagic pituitary adenomas need to be differentiated from Rathke cleft cysts (RCCs) as both of them appear bright on T1-weighted image (T1WI) owing to extracellular methemoglobin and mucoid protein, respectively. Adenomas are characterized by off-midline location, fluid-fluid level, tilting of the pituitary stalk, T2 hypointense hemosiderin rim, and internal septations, while RCCs are mostly located in the midline and often have a T2 hypointense mural nodule. Apart from these, other differentials for parasellar masses displaying high signal on T1WI are lipoma, dermoid, thrombosed aneurysm, and CP[15] (►**Fig. 3**).

Meningioma

Parasellar meningiomas can arise from tuberculum sellae, planum sphenoidale, diaphragmatic sellae, clinoid processes, sphenoid wing, CSs, or clivus. These tumors mostly occur in middle-aged females. On imaging, they appear hyperdense on noncontrast computed tomography (NCCT), iso- to hypointense on T1WI and T2WI, and show diffusion restriction on DWI. On postcontrast scan, avid homogenous enhancement is seen with linear, gradually tapering enhancement extending along dura, classically known as the "dural tail sign." Pituitary gland can be identified separately from the mass.

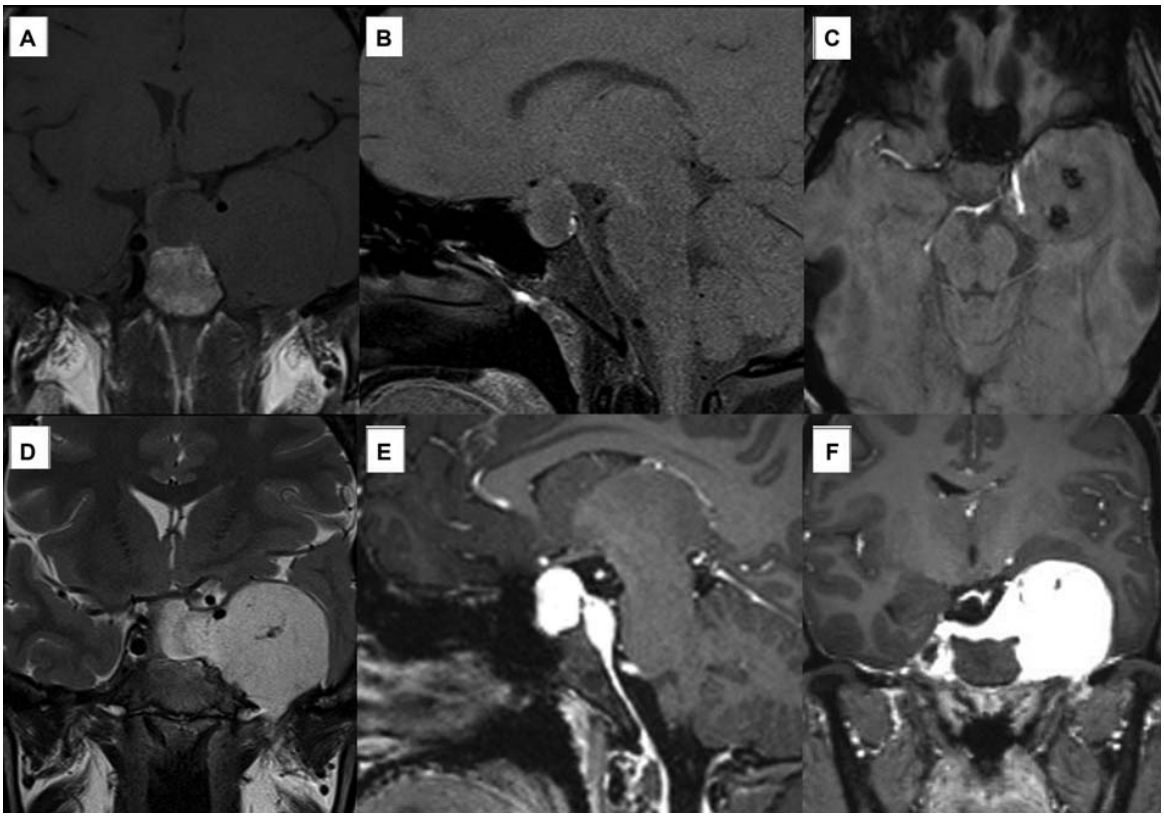

Fig. 4 In a 36-year-old lady presenting with headache and bitemporal hemianopsia, there is e/o a well-defined extra-axial mass lesion seen in region of left cavernous sinus which appears hypointense on T1-weighted image (T1WI) (**A**), hyperintense on T2WI (**D**), and shows blooming foci on gradient echo (GRE) (**C**) which appeared hypointense on filtered phase images consistent with intralesional calcification. Medially, the sella is extending into sella and causing its expansion; however, posterior pituitary bright spot is seen separately on sagittal T1WI (**B**). Compression of optic chiasm can also be appreciated (**D**). On postcontrast images, the lesion shows intense homogenous enhancement with dural tail sign (**E**, **F**). The lesion is causing encasement of the cavernous segment of left internal carotid artery (ICA) with mild luminal narrowing. On magnetic resonance (MR) spectroscopy, alanine peak was seen at 1.4 parts per million (ppm) (not shown). These findings are consistent with cavernous sinus/medial sphenoid wing meningioma.

Other ancillary signs of extra-axial tumors are also seen, namely CSF cleft, displacement of subarachnoid vessels, etc.[16] (►**Fig. 4**). Another important sign is focal hyperostosis which is better appreciated on CT scan. Meningiomas are highly vascular lesions. If diagnosis is certainly established ahead of time, tumor embolization may be performed pre-operatively that will substantially reduce intraoperative hemorrhage.[17]

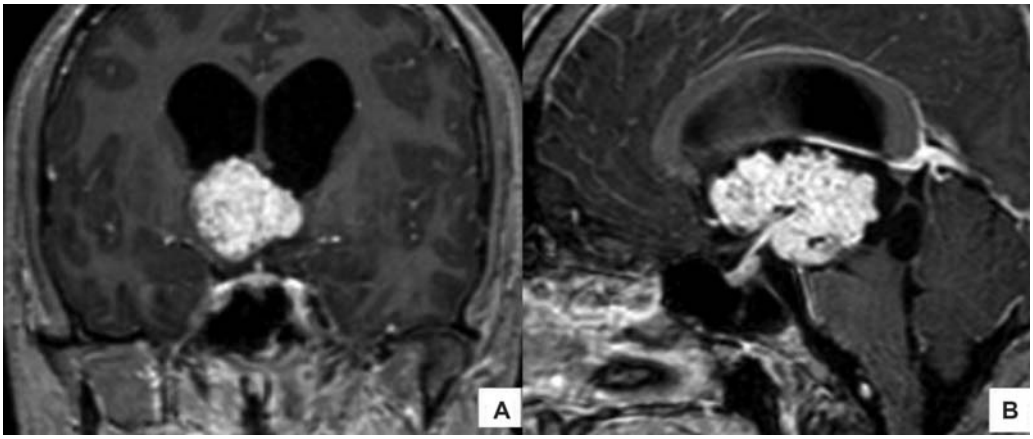

Fig. 5 Coronal and sagittal postcontrast T1-weighted image (T1WI) of a 47-year-old lady presenting with headache show a lobulated avidly enhancing predominantly solid suprasellar mass invading the third ventricle likely suggestive of papillary craniopharyngioma. Differentials include germinoma in children; intraventricular meningioma and metastases in adults.

Craniopharyngioma

CPs are the most frequently encountered nonglial neoplasms in pediatric population. These are benign, locally invasive, and nonsecreting tumors that present with clinical features related to mass effect on pituitary (hormone disturbances) or optic chiasma (visual disturbances). Majority of them are centered in the suprasellar cistern while only some of them are purely intrasellar. Rarely they may be infrasellar or intraventricular. Pathologically, they have been classified into two types. Adamantinomatous CP, the more common variant, is a lobulated mostly cystic partly solid tumor showing calcification and occurs in children aged 5 to 15 years and adults aged 45 to 60 years. Papillary CP, the less common variant that occurs in middle aged adults, is an encapsulated almost entirely solid tumor that does not usually show calcification or cystic component (►**Fig. 5**). On imaging, adamantinomatous CP appear hypodense on NCCT, hyperintense on T2/fluid-attenuated inversion recovery (FLAIR), while on T1WI they can be either hypo- or hyperintense depending on cyst contents. Lipid-lactate peak is seen on MRS owing to the cholesterol content in the cystic component. Reduced cerebral blood volume is seen on MR perfusion (►**Fig. 6**). Imaging differentials include RCC and suprasellar dermoid cyst. Enhancing solid components help differentiate them from suprasellar dermoid cyst while RCC lacks both calcification and solid enhancing components.[18]

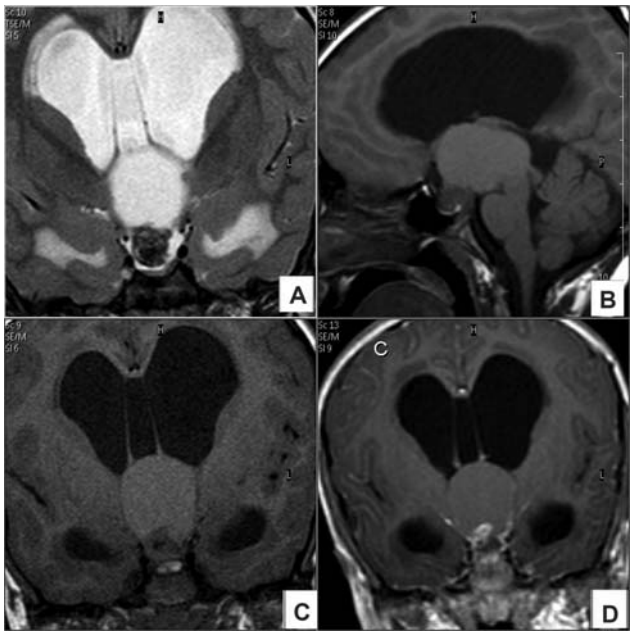

Fig. 6 Magnetic resonance (MR) images of a 9-year-old boy presenting with headache and visual disturbance show a lobulated suprasellar predominantly cystic mass lesion that is hyperintense on T2-weighted image (T2WI) (**A**) and T1WI (**B**, **C**). Solid mural nodule and cyst wall show enhancement on postcontrast images (**D**). These findings are consistent with adamantinomatous craniopharyngioma. Enhancing mural nodule helps differentiate them from Rathke cleft cyst. Noncommunicating hydrocephalus is seen due to mass effect of the lesion.

Rathke Cleft Cyst

An incidentally detected cystic lesion in a middle-aged patient in suprasellar compartment or intrasellar or both is usually a RCC. When large, it can cause symptoms due to mass effect on pituitary (hypopituitarism) or optic chiasma (visual disturbance). On imaging, they usually appear hypodense on NCCT, hyperintense on T2/FLAIR, while on T1WI they can be either hypo- or hyperintense depending on contents. On postcontrast scan, compressed pituitary is seen at the periphery of RCC as homogeneously enhancing "claw sign." Calcification is characteristically absent as opposed to CP which is the other differential for a suprasellar cystic lesion[7] (►**Fig. 7**).

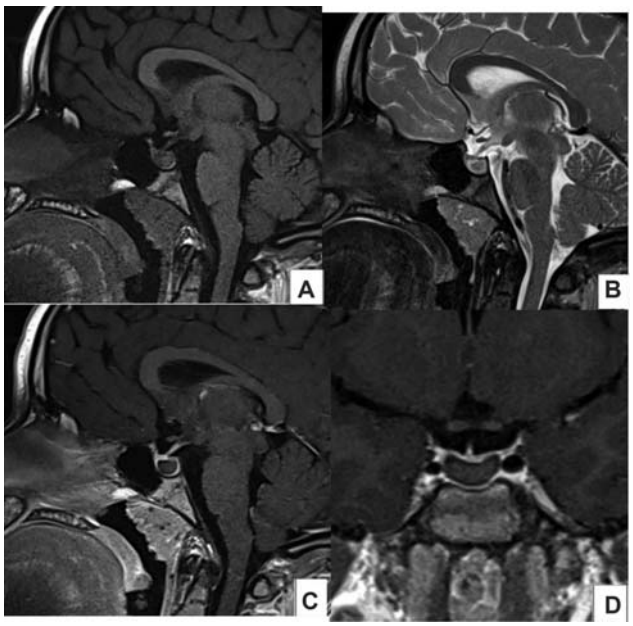

Fig. 7 Rathke cleft cyst: 3.0-T sagittal T1-weighted image (T1WI) (**A**) and T2WI (**B**) of a 42-year-old lady presenting with headaches show a well-defined intrasellar cystic lesion. Sagittal (**C**) and coronal (**D**) postcontrast T1WI show rim sign/claw sign of enhancing pituitary gland around the nonenhancing cyst.

Suprasellar Dermoid Cyst

Intracranial dermoid cysts are extremely rare, accounting for only 0.5% of all primary intracranial tumors and have a slight female predilection. On CT, it appears as a well-defined suprasellar cystic lesion with fat and calcification. On T1-weighted MRI, it shows fat-fluid level with hyperintense fat in its upper part and hypointense fluid in its lower part. Isointense nonenhancing floating round structure may be seen in its central part which has been referred to as Poke ball sign and is quite pathognomonic for dermoid cyst.[19] Uncomplicated intracranial dermoids present with mass effect. These may be complicated by rupture either spontaneous, traumatic, or iatrogenic. These patients have acute presentation, and on imaging, T1 hyperintense droplets may be seen in sulcal spaces and leptomeningeal enhancement is seen on postcontrast scan due to chemical meningitis.[20]

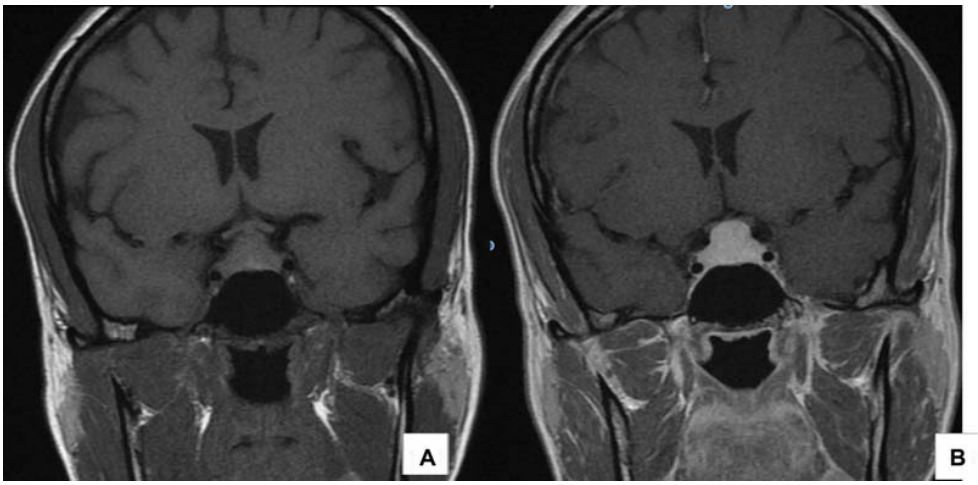

Fig. 8 Noncontrast (**A**) and contrast-enhanced (**B**) T1-weighted image (T1WI) of a prepubescent male with hypothyroidism show pathological pituitary hyperplasia with an upwardly bulging gland that mimics macroadenoma; however, it shows homogenous appearance on all pulse sequences with no discrete lesion. Reversal to normal size was seen in repeat scan done weeks after initiation of thyroid hormone replacement therapy. Physiologically, pituitary hyperplasia is seen in pregnancy and at puberty.

Pituitary Hyperplasia

Physiological variations in size of pituitary must be borne in mind. "Elster's rule" is a handy guide for assessing height of pituitary vis-a-vis patient's age. It states that the maximum upper limit for height in children is 6 mm, for men and postmenopausal ladies it is 8 mm, for women of reproductive age the limit is 10 mm, while for pregnant and lactating women, it is 12 mm. Anything exceeding this is pathological and shows upward bulging contour of the gland. This may be caused by nonneoplastic hyperplasia which mainly occurs as a response to end-organ failure, most commonly in cases of hypothyroidism and is reversible with hormone replacement therapy. On imaging, hyperplastic gland shows similar signal intensity as normal gland, appearing isointense to gray matter on both T1WI and T2WI and shows homogenous postcontrast enhancement[1] (►**Fig. 8**).

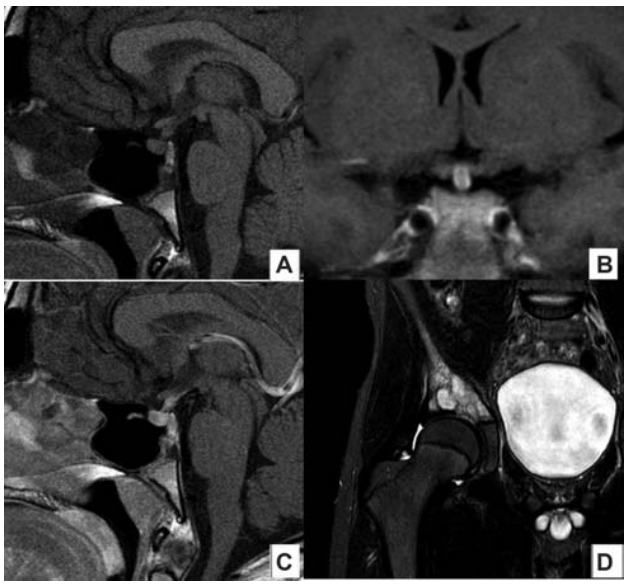

Fig. 9 Precontrast T1-weighted image (T1WI) sagittal (**A**), coronal (**B**) and sagittal (**C**) postcontrast T1WI of a patient presenting with diabetes insipidus show absent posterior pituitary bright spot (PPBS) and thick enhancing infundibulum, typical of Langerhans cell histiocytosis (LCH). Coronal T2FS of right hip (**D**) of same patient showing skeletal involvement.

Infundibulum

Normal infundibular stalk tapers craniocaudally, measuring 3.45 ± 0.56 mm at the level of optic chiasm and 1.91 ± 0.4 mm at site of insertion in pituitary.[21] Its signal intensity on T1WI is usually less than that of optic chiasma and does not normally enhance on postcontrast scan. Deviation of the stalk to one side does not necessarily suggest an underlying disease process. Infundibular lesions are often seen in children presenting with diabetes insipidus. Major differentials are Langerhans cell histiocytosis (LCH) and germinoma. Even if the scan appears normal at initial presentation, a repeat scan should be suggested after 3 to 6 months.[22]

Langerhans Cell Histiocytosis

In LCH, imaging shows a thick, enhancing nontapering stalk, often with absent posterior pituitary bright spot (PPBS). Also, look out for the classical lytic bone lesions with beveled edges[23] (►**Fig. 9**).

Germinoma

Germinomas appear as solid infiltrating masses often showing CSF dissemination. On imaging, they are hyperdense on NCCT, iso- to mildly hyperintense on T1/T2WI, and show homogenous avid postcontrast enhancement. Synchronous pineal lesion can also be seen. Tumor markers like alpha-fetoprotein or human chorionic gonadotropin in serum or CSF, if present, can help in confirming the

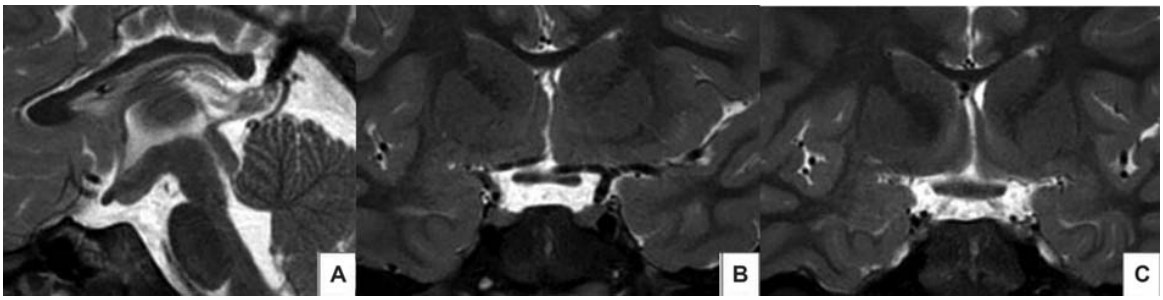

Fig. 10 Sagittal T2-weighted image (T2WI) (**A**) shows thickened floor of third ventricle from fusion of hypothalamus and an almost inapparent sella. Coronal T2WI images of the same patient show two laterally displaced pituitary glands (**B**) and duplicated pituitary stalks (**C**).

diagnosis; however, their absence does not exclude the diagnosis. They are very radiosensitive and amenable to treatment by radiotherapy. Chemotherapy is added in cases with CSF spread. Follow-up MRI is suggested for evaluation of treatment response. Germinomas are fluorodeoxyglucose (FDG)-avid, thus 18-FDG positron emission tomography scan can be used to assist in making the diagnosis or for posttreatment follow-up to look for residual or recurrent tumor.[24]

Lymphocytic Hypophysitis

It usually affects peripartum women and presents with hypopituitarism or diabetes insipidus. Major imaging differential is macroadenoma. Gutenberg et al have suggested a clinicoradiological score to help differentiate the two, as their treatment is poles apart. While macroadenoma has to be managed surgically, lymphocytic hypophysitis (LH) is usually self-limiting and can be managed conservatively with anti-inflammatory steroids and hormone replacement. Symmetrical enlargement of gland up to 6 mL, absent PPBS, enlarged stalk, homogenous appearance, intense postcontrast enhancement, and intact sellar floor are points favoring LH.[8]

Congenital Anomalies

Duplication of Pituitary Gland

Duplication of pituitary gland (DPG) is a very rare congenital anomaly with the most recent review reporting 42 cases worldwide.[25]

It may be detected in some patients presenting with anosmia, precocious puberty, or delayed onset of puberty. DPG is often associated with midline craniofacial anomalies and together they constitute DPG-plus syndrome[26] (►**Fig. 10**).

Ectopic Posterior Pituitary

Patients with ectopic undescended posterior pituitary often present with pituitary dwarfism owing to growth hormone deficiency. Sagittal midline T1 images demonstrate hypoplastic sella with an ectopically placed PPBS at the median eminence (floor of third ventricle) (►**Fig. 11**). On imaging they can be differentiated from hypothalamic lipoma by lack of fat suppression. When ectopic PPBS is associated with hypoplastic or absent anterior pituitary and infundibulum, it is referred to as pituitary stalk interruption syndrome. Numerous other abnormalities may also be associated, like septo-optic dysplasia, vermian dysplasia, Arnold-Chiari malformation, corpus callosum agenesis, holoprosencephaly,

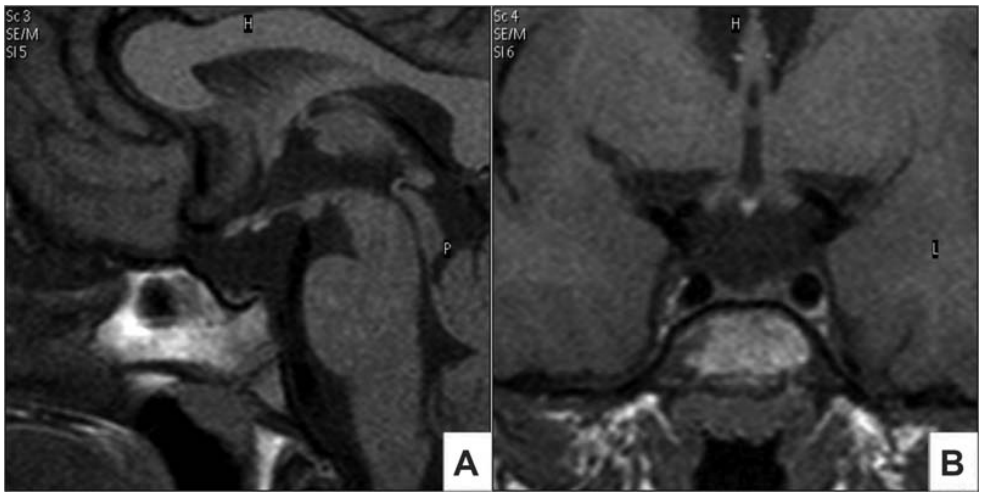

Fig. 11 3.0-T sagittal (**A**) and coronal (**B**) T1-weighted image (T1WI) of a 4-year-old girl with panhypopituitarism show ectopic posterior pituitary bright spot located along the undersurface of median eminence of hypothalamus. The infundibular stalk is absent while sella turcica and adenohypophysis are hypoplastic.

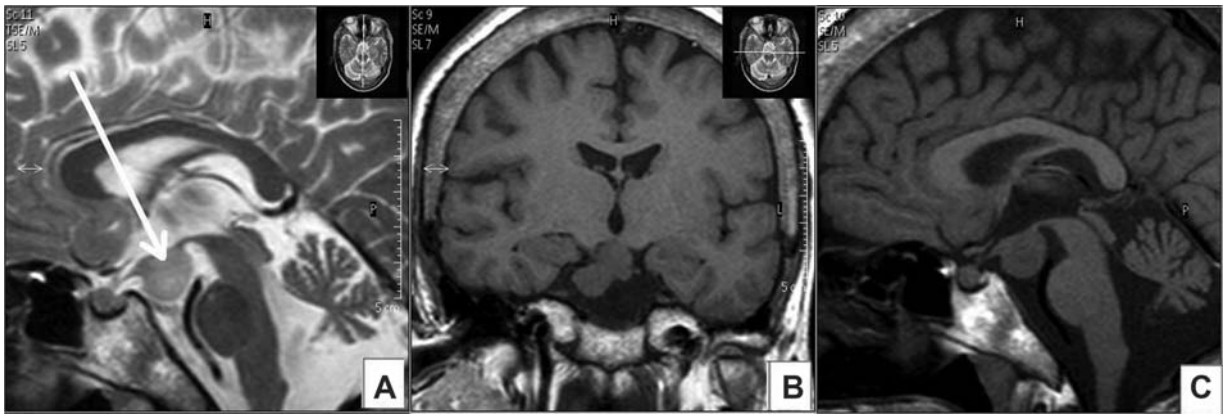

Fig. 12 Child presenting with precocious puberty. Sagittal T2-weighted image (T2WI) (**A**), coronal (**B**) and sagittal (**C**) T1WI show a pedunculated hypothalamic hamartoma appearing isointense on T1WI and iso- to slightly hyperintense on T2WI.

etc. Hence, a careful screening of the entire neuraxis should be performed.[27]

Aneurysm

Parasellar mass caused by aneurysmal dilatation of vessels shows significant signal heterogeneity with areas of T1 hyperintensity caused by subacute thrombus or flow-related enhancement or areas of T2 hypointensity caused by intracellular deoxy, or methemoglobin, calcification, or flow void. Although CPs may have significant heterogeneity, they usually have a more geographic variability from a combination of cysts, cholesterol laden lakes, and tumor tissue. Flow misregistration artifact is pathognomonic as it is not seen in other sellar masses.[28]

These aneurysms may be classified as infradiaphragmatic or supradiaphragmatic, based on their pattern of invasion into the sella and relationship to the diaphragma sellae. Infradiaphragmatic intrasellar aneurysms typically originate from the cavernous or clinoid segment of the ICA, project medially into the sella through the CS dura, tend to be smaller, and are more likely to cause hypopituitarism and CN paresis. Supradiaphragmatic intrasellar aneurysms typically originate from the ophthalmic segment of the ICA or the anterior communicating artery, are usually larger, and typically present with visual loss. It is absolutely essential to rule out a parasellar aneurysm by imaging as attempted biopsy or resection can be disastrous. Cavernous ICA aneurysms that become intrasellar carry a risk of subarachnoid hemorrhage and are best treated with endovascular techniques. Supradiaphragmatic aneurysms that cause mass effect on the visual system are likely to be preferentially treated via surgical clipping.[29]

Glioma

Glioma is the most common lesion arising from optic chiasma, commonly seen in children. Their association with neurofibromatosis 1 is well known. On imaging, it is seen as a homogeneously enhancing suprasellar mass lesion with no calcification, hemorrhage, or cystic change. Often, hypothalamus and optic chiasma both are involved and it is difficult to pinpoint the site of origin.[30]

Metastases

Metastatic lesions comprise nearly 1% of all tumors in the sellar-parasellar region. Breast and lung cancer are the two most common primaries, followed by lymphoma and prostate. Clinically, metastasis should be suspected in patients with sudden onset and rapid progression of symptoms regardless of a known primary. The possible metastatic pathways to the sella-parasellar region include leptomeningeal or hematogenous spread. Posterior pituitary is the preferred site of metastasis owing to its direct arterial supply and larger area of contact with the dura.[31]

Hypothalamic Hamartoma

They are benign nonneoplastic masses of gray matter heterotopia. Symptoms often begin in infancy and are gradually progressive. These patients present with gelastic seizures, visual problems, precocious puberty, and behavioral problems. Morphologically, these lesions can be classified into sessile and pedunculated types. As they are composed of gray matter, they have imaging appearances similar to that of the normal cortex on all sequences. They do not enhance and do not grow[32] (►**Fig. 12**).

Conclusion

To summarize, the sellar-parasellar region has a complex anatomy and can give rise to a wide spectrum of lesions that present diagnostic challenges. MRI with its multiplanar capability and excellent contrast resolution is the modality of choice for evaluation of these lesions as it not only helps in diagnostic differentiation but also provides useful information about their relationship with adjacent vital structures thereby aiding to plan appropriate treatment. Knowledge of the anatomy and proper planning of

the scan are essential for complete evaluation of sellar and parasellar pathologies.

Conflict of Interest
None declared.

References

1 Elster AD. Imaging of the sella: anatomy and pathology. Semin Ultrasound CT MR 1993;14(03):182–194
2 Sakamoto Y, Takahashi M, Korogi Y, Bussaka H, Ushio Y. Normal and abnormal pituitary glands: gadopentetate dimeglumine-enhanced MR imaging. Radiology 1991;178(02):441–445
3 Scotti G, Yu CY, Dillon WP, et al. MR imaging of cavernous sinus involvement by pituitary adenomas. AJR Am J Roentgenol 1988; 151(04):799–806
4 Yuh WT, Fisher DJ, Nguyen HD, et al. Sequential MR enhancement pattern in normal pituitary gland and in pituitary adenoma. AJNR Am J Neuroradiol 1994;15(01):101–108
5 Bonneville JF, Cattin F, Gorczyca W, Hardy J. Pituitary microadenomas: early enhancement with dynamic CT–implications of arterial blood supply and potential importance. Radiology 1993; 187(03):857–861
6 Argyropoulou MI, Kiortsis DN. Magnetization transfer imaging of the pituitary gland. Hormones (Athens) 2003;2(02):98–102
7 Osborn A, Hedlund G, Salzman K. Osborn's Brain E-Book. Philadelphia: Elsevier Health Sciences; 2017:771–817
8 Gutenberg A, Larsen J, Lupi I, Rohde V, Caturegli P. A radiologic score to distinguish autoimmune hypophysitis from nonsecreting pituitary adenoma preoperatively. AJNR Am J Neuroradiol 2009; 30(09):1766–1772
9 Cheemum L, Walter K, Walter JM, Laurence EB. The sella turcica and parasellar region. In: Magnetic Resonance Imaging of the Brain and Spine. Vol. 2;Philadelphia: WW Lippincott Co; 2002: 1283–1362
10 Dwyer AJ, Frank JA, Doppman JL, et al. Pituitary adenomas in patients with Cushing disease: initial experience with Gd-DTPA-enhanced MR imaging. Radiology 1987;163(02):421–426
11 Edal AL, Skjödt K, Nepper-Rasmussen HJ. SIPAP–a new MR classification for pituitary adenomas. Suprasellar, infrasellar, parasellar, anterior and posterior. Acta Radiol 1997;38(01):30–36
12 Knosp E, Steiner E, Kitz K, Matula C. Pituitary adenomas with invasion of the cavernous sinus space: a magnetic resonance imaging classification compared with surgical findings. Neurosurgery 1993;33(04):610–617, discussion 617–618
13 Kovacs K, Horvath E, Asa SL. Classification and pathology of pituitary tumors. In: Wilkins RH, Rengachary SS, eds. Neurosurgery. New York: McGraw-Hill; 1985:834–842
14 Pierallini A, Caramia F, Falcone C, et al. Pituitary macroadenomas: preoperative evaluation of consistency with diffusion-weighted MR imaging–initial experience. Radiology 2006;239(01):223–231
15 Park M, Lee SK, Choi J, et al. Differentiation between cystic pituitary adenomas and Rathke cleft cysts: a diagnostic model using MRI. AJNR Am J Neuroradiol 2015;36(10):1866–1873
16 Whittle IR, Smith C, Navoo P, Collie D. Meningiomas. Lancet 2004; 363(9420):1535–1543
17 Borg A, Ekanayake J, Mair R, et al. Preoperative particle and glue embolization of meningiomas: indications, results, and lessons learned from 117 consecutive patients. Neurosurgery 2013;73(2, Suppl Operative):ons244–ons251, discussion ons252
18 Sartoretti-Schefer S, Wichmann W, Aguzzi A, Valavanis A. MR differentiation of adamantinous and squamous-papillary craniopharyngiomas. AJNR Am J Neuroradiol 1997;18(01):77–87
19 Santos ARSD, de Araujo DA, Altoé A, Corrêa DG. Suprasellar mature teratoma/dermoid cyst with the Poké ball sign. Can J Neurol Sci 2021;x:1–2
20 Das CJ, Tahir M, Debnath J, et al. Ruptured intracranial dermoid. BMJ Case Rep 2009;2009:bcr2006109835b
21 Simmons GE, Suchnicki JE, Rak KM, Damiano TR. MR imaging of the pituitary stalk: size, shape, and enhancement pattern. AJR Am J Roentgenol 1992;159(02):375–377
22 Rupp D, Molitch M. Pituitary stalk lesions. Curr Opin Endocrinol Diabetes Obes 2008;15(04):339–345
23 D'Ambrosio N, Soohoo S, Warshall C, Johnson A, Karimi S. Craniofacial and intracranial manifestations of Langerhans cell histiocytosis: report of findings in 100 patients. AJR Am J Roentgenol 2008;191(02):589–597
24 Packer RJ, Cohen BH, Cooney K. Intracranial germ cell tumors. Oncologist 2000;5(04):312–320
25 Eurorad - Brought to you by the ESR. 2022. Eurorad.org. [online]. Accessed January 16, 2022 at: https://www.eurorad.org/case/17198
26 Manjila S, Miller EA, Vadera S, et al. Duplication of the pituitary gland associated with multiple blastogenesis defects: duplication of the pituitary gland (DPG)-plus syndrome. Case report and review of literature. Surg Neurol Int 2012;3(01):23
27 Kulkarni C, Moorthy S, Pullara SK, Rajeshkannan R, Unnikrishnan AG. Pituitary stalk transection syndrome: comparison of clinico-radiological features in adults and children with review of literature. Indian J Radiol Imaging 2012;22(03):182–185
28 Donovan JL, Nesbit GM. Distinction of masses involving the sella and suprasellar space: specificity of imaging features. AJR Am J Roentgenol 1996;167(03):597–603
29 Hanak BW, Zada G, Nayar VV, et al. Cerebral aneurysms with intrasellar extension: a systematic review of clinical, anatomical, and treatment characteristics. J Neurosurg 2012;116(01):164–178
30 Smith MM, Strottmann JM. Imaging of the optic nerve and visual pathways. Semin Ultrasound CT MR 2001;22(06):473–487
31 Chiang MF, Brock M, Patt S. Pituitary metastases. Neurochirurgia (Stuttg) 1990;33(04):127–131
32 Amstutz DR, Coons SW, Kerrigan JF, Rekate HL, Heiserman JE. Hypothalamic hamartomas: correlation of MR imaging and spectroscopic findings with tumor glial content. AJNR Am J Neuroradiol 2006;27(04):794–798

